Chinese Chemical Letters 36 (2025) 109841

Contents lists available at ScienceDirect

Chinese Chemical Letters

journal homepage: www.elsevier.com/locate/cclet

Light-responsive nanomaterials for biofilm removal in root canal treatment

Di An[a], Mingdong She[a], Ziyang Zhang[a], Ting Zhang[b], Miaomiao Xu[c], Jinjun Shao[a,*], Qian Shen[a,*], Xuna Tang[b,*]

[a] Key Laboratory of Flexible Electronics (KLOFE) & Institute of Advanced Materials (IAM), Nanjing Tech University, Nanjing 210009, China
[b] Department of Senior Expert Diagnosis and Treatment Center, Nanjing Stomatological Hospital, Affiliated Hospital of Medical School, Nanjing University, Nanjing 210008, China
[c] State Key Laboratory of Organic Electronics and Information Displays & Jiangsu Key Laboratory for Biosensors, Institute of Advanced Materials (IAM), Nanjing University of Posts and Telecommunications, Nanjing 210023, China

ARTICLE INFO

Article history:
Received 25 February 2024
Revised 27 March 2024
Accepted 28 March 2024
Available online 29 March 2024

Keywords:
Light-responsive nanomaterials
Biofilm
Root canal treatment
Photodynamic therapy
Photothermal therapy

ABSTRACT

Various chemical irrigants and drugs have been employed for intra-canal disinfection in root canal therapy (RCT). However, due to the complexity of root canal anatomy, many drugs still exhibit poor penetrability and antibiotic resistance, leading to suboptimal treatment outcomes. Thus, it is challenging to remove the organic biofilms from root canals. In recent years, light-responsive therapy, with deeper tissue penetration than traditional treatments, has emerged as an effective RCT modality. Herein, this review summarizes the recent development of light-responsive nanomaterials for biofilm removal in RCT. The light-responsive nanomaterials and the corresponding therapeutic methods in RCT, including photodynamic therapy (PDT), photothermal therapy (PTT), and laser-activated therapy, are highlighted. Finally, the challenges that light-responsive nanomaterials and treatment modalities will encounter to conquer the biofilm in future RCT are discussed. This review is believed to significantly accelerate the future development of light-responsive nanomaterials for RCT from bench to bedside.

1. Introduction

Bacteria in the oral cavity of humans can form biofilms on the oral tissues [1]. Bacterial biofilms are typically composed of a combination of microbial cells and organic surfaces [2]. When attached to the surface, the bacterial biofilm produces extracellular polymeric substances (EPS), providing a physical barrier to the bacteria. As a result, bacteria within the biofilm exhibit reduced sensitivity to anti-microbial drugs compared to the planktonic bacteria [3]. The biofilms in the oral cavity cause alterations in the chemical microenvironment, slowing down cell production and horizontal transfer of genes. Additionally, the biofilm matrix also protects the bacteria from nutrient deficiencies [4]. Moreover, the low pH in the microenvironment within oral biofilms significantly impedes the efficacy of antibiotics [5]. Consequently, biofilm removal is a significant clinical challenge. Persistent biofilms in the oral cavity can precipitate several conditions, including dental caries, chronic gingivitis, and periodontitis.

Root canal therapy (RCT) is a dental procedure that is now widely used in clinical practice. Its purpose is to remove the root canal of infected pulp and periapical tissues, preventing further infection and protecting the natural tooth [6]. During RCT, the infected pulp tissue is first physically cleared by specific instruments, then further cleaned and disinfected. Finally, an insert sealing material will be taken to fill in the canal space [7]. The effectiveness of RCT is influenced by various factors, including the cleaning and shaping of the root canal, as well as the controlling microbial growth. Challenges like the intricate shape of the root canal and the difficulty in eliminating specific bacteria result in a reported success rate for RCT of 70% or less, with the potential for recurrent infections [8].

To effectively remove the biofilm in RCT, physical preparation and chemical disinfection are the primary methods currently employed. However, relying solely on instrumental debridement is insufficient to completely clear the pulp tissue, debris, and bacterial biofilm of the root canal. To address this issue, irrigation plays a vital role in RCT, and anti-microbial irrigation agents can efficiently

* Corresponding authors.
E-mail addresses: iamjjshao@njtech.edu.cn (J. Shao), iamqshen@njtech.edu.cn (Q. Shen), xunatang@126.com (X. Tang).

https://doi.org/10.1016/j.cclet.2024.109841
1001-8417/

enhance the removal of root canal biofilm [9]. Common root canal irrigants include sodium hypochlorite (NaClO) and chlorhexidine (CHX), of which NaClO is the most frequently utilized irrigant in RCT [10]. NaClO can kill bacteria and dissolve necrotic bacterial tissue and microbial biofilms, and the anti-biofilm effect of NaClO increases with its concentration [11]. However, the high concentration of NaClO exhibits high cytotoxicity that negatively affects dentin at the same time [12]. Generally, the recommended concentration range of NaClO for clinical application is around 1%–6% [13]. Nonetheless, the low-concentration NaClO significantly reduces the effectiveness in the removal of root canal biofilm. CHX is another commonly used irrigant, exhibiting an excellent antibacterial effect. Owing to the positive charge feature of CHX, it can interact with the matrix components of the biofilm to modify the permeability barrier of the bacterial cytoplasmic membrane, resulting in cell rupture [14]. Moreover, CHX with a concentration of 2% achieves a remarkable anti-bacteria efficacy against *Enterococcus faecalis* (*E. faecalis*) in RCT [15]. However, CHX presents less antibacterial effectiveness in disinfecting bacteria deep-seated in the biofilm, limiting its role in root canal disinfection [16]. Overall, despite the conventional rinsing agents of NaClO and CHX that have been widely used in the disinfection stage of RCT, they demonstrate a limited capability to remove bacteria from biofilms effectively. Consequently, they are now frequently utilized in combination with other agents in RCT to augment the anti-microbial effect.

In addition to the weak biofilm-scavenging activity, NaClO and CHX exhibit certain biotoxicity at high concentrations and restricted penetration to dentin tubules [17]. Generally, the penetration depth of NaClO was around 40–309 μm, whereas *E. faecalis*, notorious for its resistance to removal during endodontic treatment, can infiltrate dentin tubules with a depth of up to 800 μm, thus generating biofilms under malnutrition conditions [18–20]. As a result, this underscores the development of novel approaches in endodontic treatment to amplify the effectiveness of traditional chemical-mechanical root canal preparation.

Recently, phototherapy and high-power laser treatment have emerged as novel approaches to address the root canal biofilm infection. Light with enhanced tissue penetration depth is believed to reach the dentin tissues inaccessible to conventional techniques [21–25]. Generally, light-induced phototherapy primarily encompasses photodynamic therapy (PDT) and photothermal therapy (PTT) [26–28]. The mechanism of PDT is shown in Fig. 1, once the photosensitizer is photo-excited after photoirradiation, it will transition from the ground state ^{0}[PS] to the excited singlet state ^{1}[PS]. Through intersystem crossing (ISC), ^{1}[PS] with a short lifetime and high activity will relax into the triplet excited state ^{3}[PS] with a relatively long lifetime. In type I PDT, the triple excited state photosensitizer ^{3}[PS] undergoes electron transfer reactions to interact with the substrate to generate highly reactive oxygen species (ROS), including hydroxy radical (·OH), superoxide anion ($O_2{\cdot}^-$), and H_2O_2 [29,30]. As for type II PDT, ^{3}[PS] goes through the energy transfer process to interact with the tissue

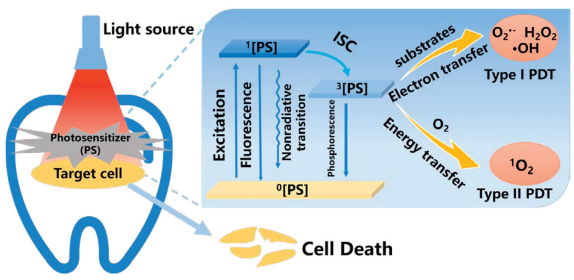

Fig. 1. Photodynamic process for root canal treatment.

oxygen ($^{3}O_2$) for singlet oxygen ($^{1}O_2$) production. Significantly, as-generated ROS can accomplish the anti-bactericidal effect through a range of multi-targeted actions, including oxidizing bacterial membranes and DNA, altering membrane permeability, deactivating membrane transport systems, and inhibiting enzymatic activity within the bacterial membranes. Therefore, PDT shows the advantages of low drug resistance with adequate anti-bacterial effects [31–33]. In addition, ^{1}[PS] can also relax to the ground state ^{0}[PS] *via* non-radiative decay to produce hyperthermia for PTT [34–37]. In RCT, PTT can elevate the temperature inside the root canal, and effectively kill or inactivate bacteria and potential pathogens, thus mitigating the risk of infection within the dental root canal.

Moreover, the development of nanoplatforms is also imperative to penetrate the biofilm barrier, enhance water solubility, and refine drug targeting [38]. The construction of nanoplatforms is believed to be an up-and-coming biofilm removal method. Through modulation of size, surface charge, and shape, light-responsive nanomaterials can bolster their anti-bacterial efficacy against biofilms in RCT. This approach offers unmatched flexibility in transporting, holding, and releasing drugs precisely when and where they are required. Furthermore, nanoparticle-based drug delivery systems shield traditional medications from pH or enzymatic degradation in challenging biofilm environments. The innate high surface area-to-volume ratio of nanoparticles facilitates their carriage of multiple drugs, leading to a synergistic therapy against bacterial biofilm [39–44].

Due to the intricate structure of root canals, it is a significant challenge to remove the biofilm. Light-activated treatment approaches offer distinctive advantages in RCT, including deep penetration depth, high treatment efficacy, and low drug resistance. Therefore, numerous light-responsive nanomaterials and their therapeutic modalities in RCT have garnered significant research attention recently. In this review, the recent advance of light-responsive nanomaterials for biofilm removal in RCT is summarized (Table 1 [45–60]). Meanwhile, the corresponding therapy methods of light-responsive nanomaterials in RCT are highlighted, including PDT, PTT, and laser-activated therapy. The challenges of the light-responsive nanomaterials and treatment modalities in RCT are also discussed. It is hoped that this will guide the future development of light-responsive nanomaterials for biofilm removal in RCT.

2. PDT

There are three vital elements in PDT, including light source, photosensitizer, and tissue oxygen [61]. Photosensitizers play a vital role in light-absorption and ROS generation for anti-microbial PDT, and they can bind to the outer surface, cell membrane, and DNA of microorganisms, thereafter becoming activated to produce ROS upon light-irradiation [62]. The photosensitizers applied in RCT should take into account several factors below. Firstly, photosensitizers should have good photostability. The wavelength of the photosensitizer should be located in the biological therapeutic window (600–800 nm) since wavelengths shorter than 600 nm penetrate tissues less effectively penetration and exhibit a higher risk of photobleaching. Additionally, photosensitizers should also possess considerable ease for highly efficient ROS generation upon photoirradiation. Finally, photosensitizers should have high biosafety and can be easily eliminated from the root canal to minimize the adverse effects. The photosensitizers currently used in RCT with PDT are presented in Fig. 2.

2.1. Methylene blue (MB)

MB, a colored photosensitizer, is widely applied in clinical dentistry (Fig. 2A) [63]. MB belongs to the phenothiazine family of photosensitizers, with an absorption peak around 660 nm [64]. Due

Table 1
Summary of the light-responsive nanomaterials of biofilm removal in RCT.

Therapy	Nanomaterials	$\lambda_{max}{}^{abs}$ (nm)	Microorganism or model	Novelty of strategy or therapeutic effect	Refs.
PDT	Methylene blue	660	*E. faecalis*	Addition of KI was employed with MB	[45]
PDT	Methylene blue	660	*E. faecalis*	QCh triple-layer structure	[46]
PDT	Toluidine blue	630	*E. faecalis*	TB-mediated PDT as an adjunctive treatment modality	[47]
PDT	Toluidine blue	630	Saliva-derived multispecies biofilms	Magnetic field as the navigation	[48]
PDT	Indocyanine green	810	*E. faecalis*.	ICG loaded onto nano-graphene oxide	[49]
PDT	Indocyanine green	810	*E. faecalis*	Chitosan-loaded ICG nanospheres	[50]
PDT	Curcumin	420	*E. faecalis*	Nano curcumin with LED and SWEEPS	[51]
PDT	Curcumin	420	*E. faecalis*	Mixing Curcumin into polymer fibers	[52]
PDT	Emodin	434	*E. faecalis*	Apt and DCD-1 L to improve targeting	[53]
PDT	Rose Bengal	550	Multiple bacteria model	Cationic polymer with quaternary ammonium and dextran	[54]
PDT	DPA-SCP (AIE)	440	*E. faecalis*	DAP-SCP-mediated PDT could achieve the same effect as 1% NaClO	[55]
PDT	Ce6/CaO_2/ZIF-8@PEI	660	*E. faecalis*	Oxygen self-supplied nanoplatform	[56]
PTT	PBDT-DIID NPs	776	*E. faecalis*	Low-concentration NaClO solution, heated by PBDT-DIID NPs	[57]
PTT	MPN-Pd	808	Multiple bacteria model	Combining oxidase-like and photothermal properties	[58]
PTT	Au@$Cu_{2-x}S$	808	Isolated dental slices, root canal models, and beagle dog	PTT and PCT	[59]
Laser activation irrigation	Er,Cr:YSGG laser activation		*E. faecalis*	Low concentrations of NaClO, activated by Er,Cr:YSGG LAI	[60]

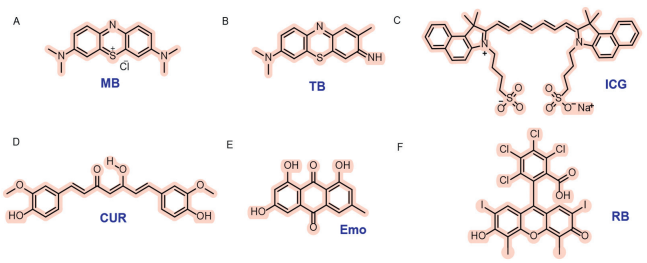

Fig. 2. Chemical structure of the photosensitizers: (A) methylene blue (MB), (B) toluidine blue (TB), (C) indocyanine green (ICG), and (D) curcumin (CUR), (E) emodin (Emo). (F) Rose Bengal (RB).

to its positive charge from the central S atom and its hydrophilic nature, MB can easily pass through the cell membranes of oral bacteria [65]. Moreover, MB presents prominent biocompatibility and reduced cytotoxicity toward human gingival fibroblasts and osteoblasts [66]. However, since photosensitizer MB is a colored dye, the dental structures may eventually be stained [67]. In addition, hydrogen bonding may also promote the stabilization of collagen fibers after MB staining, which further exacerbates the pigmentation of dental substrate [68].

To mitigate tooth staining, potassium iodide (KI) was employed with MB together to enhance the photobleaching effect and minimize the MB staining [45]. The bactericidal impact of photoactivated MB in conjunction with KI against *E. faecalis* in both planktonic and biofilm forms was investigated. It was found that 10 μmol/L MB photoactivation + KI could offer a more practical approach for biofilm eradication. This combination effectively disinfected bacterial biofilms formed on human teeth and sustained the bactericidal effect after the light was turned off. In addition, it could remain bactericidal in the presence of hypoxia. In the hypoxia microenvironment, the anti-bacterial effect PDT with MB alone was entirely ineffective, though the MB with the addition of KI retained some anti-bacterial activity although the killing results were not good as that found in the presence of oxygen. A possible explanation is that the photoactivated MB could engage in oxygen-independent electron transfer reactions, leading to the generation of iodine radicals from iodide anions. This innovative study demonstrated that the incorporation of KI with MB during PDT increased free iodine and hydrogen peroxide (H_2O_2) production. H_2O_2 is an efficient bactericidal agent, and its coexistence with free iodine may be account for the continuous sustained antibacterial effect, even post-illumination. Therefore, PDT combined with MB + KI holds an excellent potential for root canal disinfection; thus, its clinical study is worth promoting.

In addition, to improve the targeting selectivity and anti-biofilm properties of photosensitizer MB, a triple-layer nanostructure was rationally designed, in which MB was encapsulated within quaternary ammonium-decorated chitosan (QCh) modified upconversion nanoparticles (UCNPs)@SiO_2/MB@QCh [46]. Lanthanide-doped UCNPs served as carriers for MB, and a layer of silicon dioxide was applied on their surfaces to carry the MB, which constituted UCNP@SiO_2/MB. Subsequently, QCh was applied to UCNP@SiO_2/MB as a coating. Due to its superb water solubility, QCh was presumed to enhance the conversion efficiency of UCNPs, leading to the production of a more significant amount of ROS [69]. More importantly, Qch could augment the interaction between UCNP@SiO_2/MB@QCh and *E. faecalis* through electrostatic interaction. Then, UCNP@SiO_2/MB@QCh generated ROS in close proximity to *E. faecalis* under 980 nm laser irradiation (Fig. 3). More than 99% of *E. faecalis* was cleared by UCNP@SiO_2/MB@QCh during PDT, and this superior anti-microbial activity was attributed to the firm adherence of QCh to the bacteria. QCh could adsorb bacteria and compromise their cell membranes, resulting in the expulsion of DNA and RNA from the cytoplasm and thereby effectuating bacterial destruction. In synergy with the activity of ROS, UCNP@SiO_2/MB@QCh accomplished a dual anti-bacterial action. Furthermore, as a well-known biocompatible and non-toxic material, the QCh integration significantly diminished the toxicity of photosensitizers and enhanced their biosafety, making them extensively applicable in biological fields [70]. This study paves the way for new avenues in employing nanotechnology and PDT to address persistent infections, particularly within root canal treatments.

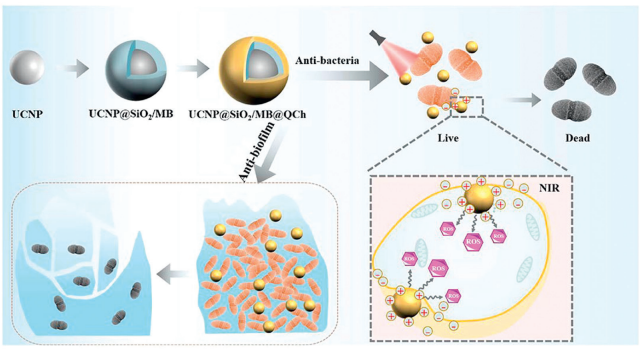

Fig. 3. Preparation of UCNP@SiO_2/MB@QCh and the anti-bacterial effect. Copied with permission [46]. Copyright 2022, Frontiers.

2.2. Toluidine blue (TB)

TB is another commonly used phenothiazine salt photosensitizer in endodontic treatment (Fig. 2B). TB exhibits a similar absorption spectrum to MB, with a peak at around 630 nm [71]. It binds to the polyphosphate on bacterial outer membranes, thus damaging the lipids and proteins. The reactivity of TB with cell membranes amplifies with increasing hydrophobicity since TB is more soluble in the cell membrane's hydrophobic region. Consequently, TB serves as a superior photosensitizer for membrane targeting [72,73].

The anti-microbial efficacy of PDT based on TB was assessed on extracted teeth previously infected with *E. faecalis* biofilm [47]. Fifty-four extracted single-tube teeth were processed, sterilized, autoclaved, and inoculated with *E. faecalis*. The treated teeth were then grouped into six categories: two each for negative and positive controls, mechanical instrumentation combined with varied PDT pre-irradiation timings, and chemo-mechanical cleaning combined with different PDT pre-irradiation and irradiation durations. For the PDT group, following the TB application, a diode laser (635 nm wavelength, 200 μm fiber diameter, 100 mW) was employed to irradiate the canals continuously, and a notable bacterial reduction was found by using PDT combined with chemo-mechanical treatment. This study indicated the great potential of PDT as a supplementary treatment to enhance the disinfection of *E. faecalis* biofilm.

Moreover, to address the challenge that the dense structure of biofilm for limited penetration, a multi-functional nanoplatform MagTBO, combining photosensitizer *ortho*-toluidine-blue (TBO) with superparamagnetic iron oxide (Fe_2O_3) NPs was developed for PDT against dental caries-related biofilms [48]. The PDT efficacy in combating Streptococcus mutans (*S. mutans*) and saliva-derived multispecies biofilms showed marked improvement. Capitalized on an external magnetic field as the driving force, MagTBO nanoplatform demonstrated superior biofilm penetration and an enhanced PDT sterilization effect. In addition, MagTBO exhibited commendable water solubility, photostability, and biocompatibility. This study reveals that incorporating a magnetic field and magnetic nanoparticles for targeted PDT can significantly improve the anti-biofilm therapeutic effect, offering a novel approach to RCT.

2.3. Indocyanine green (ICG)

ICG is an anionic photosensitizer with near-infrared (NIR) absorption peaked at 810 nm (Fig. 2C), and it has received approval from the U.S. Food and Drug Administration (FDA) for clinical imaging [74]. ICG has been reported as a novel photosensitizer that shows significant anti-bacterial activity against *E. faecalis* [75]. Additionally, ICG possesses a longer wavelength compared to other photosensitizers utilized in RCT, enabling deeper penetration [76]. Moreover, its specific absorption peak coincides with commercially available dental laser diodes of 808 nm, making it more economically advantageous than other photosensitizers.

As a negatively charged photosensitizer, ICG interacts weakly with the similarly negatively charged surfaces of microorganisms [77]. Furthermore, ICG is prone to concentration-dependent aggregation in aqueous solutions and exhibits poor targeting capabilities. To improve the ICG binding to microorganisms, nano-graphene oxide (NGO) was employed as the carrier for the preparation of NGO-ICG nanocomposites for enhanced PDT [49]. The high specific surface area of NGO enabled the sufficient adsorption of ICG molecules, remarkedly enhancing the stability of ICG and amplifying the PDT effect. Ultimately, NGO-ICG-mediated PDT considerably diminished the biofilm formation of *E. faecalis*. Despite the ICG concentration within NGO-ICG being one-fifth of traditional PDT, it notably decreased the *E. faecalis* count. Furthermore, with a reduced final ICG concentration (1/5), NGO-ICG-based PDT exhibited anti-membrane activity 1.3 times greater than its ICG-only counterpart. This novel NIR light-responsive drug delivery system provides the benefits of cost-efficiency, reduced dye concentration exposure, minimal tooth discoloration, and anti-biofilm.

Another way to improve ICG interaction with cells is to take advantage of the positive charge properties. Through taking a diode laser as the light source, ICG-loaded nanospheres ICG-Nano/c with ICG-loading and chitosan-coating were developed to target the biofilm of *E. faecalis* for anti-bacterial PDT towards refractory periapical radiculitis [50]. The chitosan coating imparted a positive charge to the photosensitizer, enhancing its affinity for negatively charged bacteria. The final results demonstrated over a 98% reduction in viable cells of *E. faecalis*, and there was no unsafe temperature increase in the root canal. Scanning electron microscopy (SEM) confirmed the impact of ROS in the diminishing *E. faecalis* biofilm, resulting in a substantial decrease in the biofilm on the dentin surface, although a complete biofilm removal was not achieved. Chitosan was believed to be capable of breaking down the extracellular polymeric substances, thereby disrupting the architecture of bacterial biofilm. In addition, the magnitude of the transmitted energy of the laser after passing through empty root canals and saline was compared. Once ICG-Nano/c absorbed the light energy upon irradiation, the absorbance gradually decreased over time. This may be due to the fact that ICG was easily photobleachable and would decompose upon light illumination. Under illumination, the polymethyl chain of ICG would form a dioxane ring, which could produce singlet oxygen that further decompose into carbonylated molecules. Thus, the absorption decline was supposed to stem from the decomposition of ICG-Nano/c after irradiation, leading to a progressive deterioration in its photosensitizer functionality.

2.4. Curcumin (CUR)

CUR, as an anti-bacterial, anti-inflammatory, and non-toxic agent, is a natural hydrophobic phenolic compound derived from plants (Fig. 2D) [78,79]. Within the realm of dentistry, CUR serves as a photosensitizer for PDT with an absorption peak at 420 nm. There are reports suggesting that the PDT reaction of CUR may not be related to the generation of $^1O_2$, but it could be associated with the production of other active compounds [80]. Due to its remarkable photodynamic activity, it has garnered attention from various phototherapy research groups [51].

The PDT effectiveness of photosensitizer CUR and other photosensitizers (TB, MB, ICG) in RCT for the eradication of *E. faecalis* biofilms was examined for comparison [71]. Among these photosensitizers, CUR displayed superior capabilities in inhibiting biofilm formation, and the potent anti-biofilm prowess of CUR was likely

attributed to its ability to destabilize bacterial cell membranes by hindering the FtsZ assembly kinetics with the z-ring [81]. In addition, CUR, a hydrophobic compound, could alleviate the association with water, and it owned a low affinity for glycoproteins in collagen fibers, both of which were anionic [82]. Therefore, another critical advantage of CUR as a photosensitizer in endodontic treatment is that it has less impact on tooth discoloration after use [83].

Despite its commendable anti-bacterial and anti-biofilm attributes, the clinical adoption of CUR remains constrained, mainly due to its suboptimal solubility and unstable hydrolysis [84]. Therefore, to overcome the limitation of the clinical application, CUR nanoparticles with large surface area and positive charge were developed for anti-bacterial therapy [85]. They could readily interact with bacterial cell walls bearing a negative charge to exert anti-bacterial effects [86].

E. faecalis within the root canal of extracted teeth was eliminated utilizing shock wave enhanced emission photoacoustic streaming (SWEEPS) technology together with CUR, nano-curcumin photosensitizer, and light emitting diode (LED)-assisted PDT [51]. The combination of nano-curcumin, LED, and SWEEPS demonstrated the most pronounced anti-bacterial activity. SWEEPS, a relatively recent development in Er:YAG laser-assisted irrigation, employs laser pulses to initiate a bubble flow. This method produces potent shock waves, amplifying acoustic streaming [87]. Amplifying the generation of shockwaves coupled with optically activated acoustic streaming enables the removal of infectious agents from challenging areas within the root canal, enhancing the efficacy of root canal irrigation. The amplified anti-bacterial efficacy from the LED and SWEEPS combo could be ascribed to the divergent and incoherent nature of LED beams. When used in conjunction with PDT, the LED ensures microbial cells receive irradiation from multiple angles, leading to membrane disruption and facilitating light penetration into these cells [88].

In addition to the anti-microbial treatment with CUR in the form of nanoparticles, Julian's group mixed CUR into polymer fibers to investigate its anti-bacterial properties and its potential application in root canal disinfection [52]. Electrospinning is a significant drug delivery technique that allows for the incorporation of multiple drugs into a single phase, facilitating synergistic therapy [89]. Continuous disinfection of root canals was achieved by using light-activated, low-concentrated electrospun curcumin-modified fibers. While Curcumin's anti-bacterial efficacy in the study did not surpass that of the positive control NaClO, it is worth noting that NaClO is not biocompatible and can potentially diminish the survival rate of pulp stem cells. Hence, CUR exhibits promising potential for RCT.

2.5. Emodin (Emo)

Apart from CUR, Emo is another plant-sourced organic compound exhibiting photosensitizing characteristics (Fig. 2E) [90]. Exhibiting an excitation wavelength of 434 nm [91], it presents as a reddish-orange powder or crystal within the anthraquinone family. This compound possesses multiple advantageous pharmacological activities, encompassing anti-inflammatory, antioxidant, anticancer, and immunomodulatory properties [92]. Studies indicate that emodin nanoparticle (EmoNP) inhibits biofilm formation, degrades established biofilms, and functions as a virulence factor, diminishing biofilms across various bacterial strains [93]. However, it has been reported that emodin may have toxic effects on healthy cells [94], so its current application is still limited, and it is rarely reported in the dental field.

To mitigate this concern, researchers harnessed the aptamer's high selectivity to engineer the Apt@EmoNp-DCD-1L complex [53]. This design was aimed to target *E. faecalis,* specifically, sparing non-target cells from destruction. Apt served as a selective agent for *E. faecalis*. Aptamer, a small single-stranded DNA or RNA molecule, exhibited strong binding affinity and specificity to its target molecules [95]. Furthermore, PDT targeting could be improved by incorporating DCD-1L, an amphiphilic peptide characterized by a cationic end and an anionic c-terminal. This peptide exhibited extensive anti-microbial activity. Studies demonstrated that DCD-1L binds to negatively charged bacterial phospholipids, initiating the formation of zinc ion-dependent oligomers within bacterial membranes. This interaction subsequently resulted in the establishment of ion channels and membrane depolarization, culminating in bacterial cell demise.

E. faecalis dominates as the primary pathogen in the root canal system, deriving its pathogenicity from multiple encoding virulence factors. The virulence factors empower *E. faecalis* to establish colonization, elude immune responses, and form biofilm [96]. During PDT process, the photosensitizer EmoNp possessed the capability to associate with proteins related to encoding virulence factors, thereby impeding the formation and existence of *E. faecalis* biofilm. Quantitative real-time PCR data revealed that PDT employing Apt@EmoNp-DCD-1L effectively down-regulated the expression of genes associated with biofilm formation. Notably, the reduction of gene expression in the PDT group mirrored that in the 0.2% CHX group, showcasing no significant disparity. This implied that PDT's efficacy in downregulating virulence genes is comparable to that of 0.2% CHX, underscoring PDT's notable effectiveness without accompanying side effects. By combining *E. faecalis*-targeted Apt@EmoNp-DCD-1L with photoirradiation, the growth of *E. faecalis* in biofilm forms could be effectively inhibited. In addition, the antitoxic activity of Apt@EmoNp-DCD-1L-mediated PDT indicated that the gene expression levels involved in bacterial biofilm formation were exceptionally reduced. Consequently, nanoplatform Apt@EmoNp-DCD-1L holds the potential for targeting a wide range of biofilm-forming microorganisms.

2.6. Rose Bengal (RB)

RB, a dark red xanthene photosensitizer (Fig. 2F), exhibits an absorption spectrum spanning 500 nm to 580 nm, peaking at 550 nm, and is known for its high singlet oxygen generation [97]. RB is mainly considered as a diagnostic tool in ophthalmology, and demonstrates inherent cytotoxicity towards most tumors and microbial cells, highlighting its potential in the biomedical field. However, there are some limitations to its use as a photosensitizer. Firstly, RB is a compound with high water solubility. Owing to the lipophilic nature of the cell membrane, a pharmaceutical agent requires lipophilicity to facilitate its spontaneous transmembrane passage and subsequent re-localization within the intracellular organelles. The poor lipophilicity of RB hinders its ability to traverse the cell membrane, resulting in weak intracellular uptake and consequently, a suboptimal phototherapeutic effect. Moreover, the short half-life of RB is also a barrier to the normal accumulation, and necessitating multiple administrations to achieve the therapeutic threshold. Furthermore, at physiological pH, RB carries a negative charge and thus interacts weakly with the negatively charged cell membranes, which impedes its cellular absorption [98].

Taking functionalized RB as a photosensitive unit, polymeric photosensitizer HQRB-SS-Dex was exploited for PDT against a wide range of oral bacteria (Fig. 4) [54]. Under light irradiation, photosensitizer HQRB-SS-Dex scavenged *Porphyromonas gingivalis* (*P. gingivalis*), *Actinobacillus actinomycetemcomitans* (*A. actinomycetemcomitans*) anaerobic bacteria, and facultative anaerobic *S. mutans*. To maximize the utilization of ROS generated by photosensitizer RB under light exposure, positively charged quaternary ammonium derivatives were employed to link RB and the negatively charged bacteria tightly together. The polysaccharide dextran in photosen-

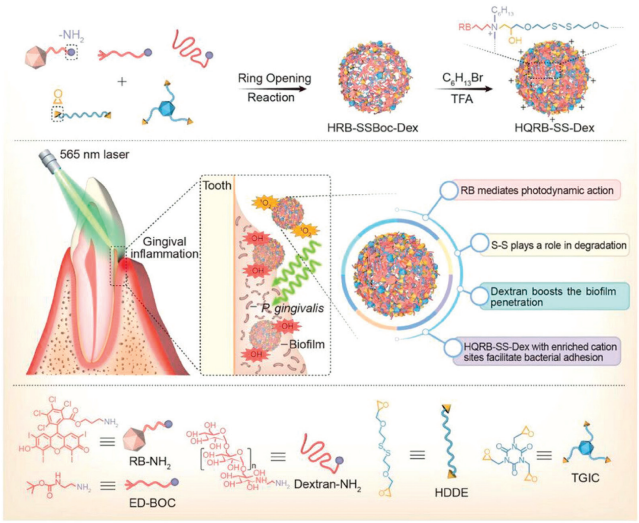

Fig. 4. Synthesis pathway for polycationic anti-bacterial agents with multi-functional components and their application in PDT for periodontitis. Copied with permission [54]. Copyright 2023, Wiley-VCH GmbH.

sitizer HQRB-SS-Dex rendered a superior binding to bacteria and biofilms which featured with overexpressed nonenzymatic lectins, allowing further deep penetration into the biofilms. Furthermore, upon photoirradiation, HQRB-SS-Dex generated $^1O_2$ and ·OH simultaneously through type I and type II photodynamic pathways, leading to outstanding anti-bacteria effect and significant biofilm disintegration. Additionally, glutathione (GSH)-sensitive disulfide bonds (-SS-) were implemented to endow the branched polymer HQRB-SS-Dex with outstanding biodegradability and excellent biosafety.

2.7. Other photosensitizers

Beyond the above commonly used photosensitizers in RCT, several innovative photosensitizers are also employed. These are anticipated to expand the options for future RCT. The bacterial inhibitory effect of currently used photosensitizers in endodontic treatment is lower than that of NaClO, and they generally suffer from poor stability, weak ROS generation, and the propensity to stain teeth [99]. Meanwhile, conventional organic photosensitizers suffer from aggregation-caused quenching (ACQ). As aggregation increases, the fluorescence intensity of traditional fluorescent molecules diminishes, reaching an almost complete quench in the solid state [100]. In 2001, a phenomenon contrasting with ACQ was identified by Tang *et al*. and termed “aggregation-induced emission” (AIE). Photosensitizers with AIE properties exhibit high stability and ROS production capacity. In addition, AIE photosensitizers also possess excellent imaging properties and anti-bacterial ability, which are expected to play an essential role in endodontic treatment.

The AIE photosensitizer DPA-SCP was innovatively developed for PDT against the *E. faecalis* suspension, through the evaluation of bacteriostatic activity in the growth of the bacterial suspension (Fig. 5A) [55]. AIE photosensitizer DPA-SCP demonstrated qualities such as high photosensitivity, minimal toxicity, and good photostability. Its absorption peak is around 440 nm. *E. faecalis* biofilms were first cultured in the root canal lining and successfully developed into a biological root canal infection model (Fig. 5C). This model was then subjected to DPA-SCP-mediated PDT. DPA-SCP-mediated PDT demonstrated a significant germicidal effect on *E. faecalis* suspensions and 21-day biofilms in human root canals, achieving the same effect as 1% NaClO. In addition, the DPA-SCP-mediated PDT showed no apparent chemical corrosivity and significantly lower cytotoxicity, in contrast to NaClO. It is the first work to apply AIE photosensitizer to a model of root canal biofilm infection, and the excellent anti-bacterial effect showed that AIE photosensitizer held promise as an effective clinical disinfection strategy in dentistry.

Oxygen is a crucial factor influencing the effectiveness of PDT [101]. The anoxic complexity of the root canal system dramatically reduces the PDT efficacy, especially for type II PDT that relies on oxygen for $^1O_2$ production [102]. Therefore, a cationic self-oxygenated nanoplatform was constructed to combat *E. faecalis* biofilm effectively. A nanoplatform Ce6/CaO_2/ZIF-8@polyethylenimine (PEI) was developed to enhance PDT (Figs. 5B and D) [56]. PEI offered a positively charged surface, enhancing its targeting precision for bacteria. The reaction of CaO_2 with H_2O generated the O_2 substrate necessary for Ce6 photodynamic processes, significantly enhancing the phototoxic effects of photosensitizer Ce6 under 660 nm irradiation (Fig. 5E). This nanoplatform had been proven to cause cell membrane damage, nucleic acid leakage, and ROS metabolism abnormalities in plankton bacteria. *In situ* anti-bacterial results further validated its effect on the diffusion and elimination of mature intratubular and intratubular bacterial biofilm. This innovative design presents a practical solution for ameliorating hypoxia in the root canal system, addressing the limitations of photosensitizers and opening new avenues for treating persistent root canal infections.

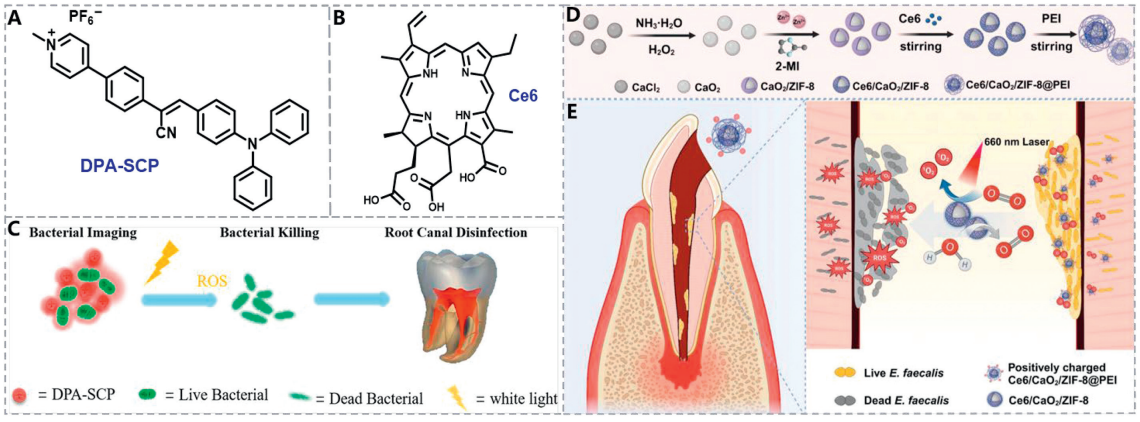

Fig. 5. Chemical structures of (A) DPA-SCP and (B) Ce6. (C) Photosensitizer DPA-SCP for bacterial imaging, bacterial killing, and root canal disinfection. Reproduced with permission [55]. Copyright 2021, American Chemical Society. (D) Assembly of Ce6/CaO_2/ZIF-8@PEI nanoplatform and its targeted antibiofilm efficacy against root canal infections. (E) PDT of Ce6/CaO_2/ZIF-8@PEI NPs on *E. faecalis* under 660 nm irradiation. Reproduced with permission [56]. Copyright 2024, Wiley-VCH Gmb.

2.8. Removal of photosensitizer

The previous section provided a discussion of the available photosensitizers in RCT. Nevertheless, it is essential to note that photosensitizers with high viscosity can penetrate the dentin surface extensively. It may form a chemical smear layer, which might induce the blockage of dentin tubules, resulting in microleakage and diminished adhesive force between the root canal dentin and the filling material [103]. Specifically, certain photosensitizers as dyes, such as MB and TB, can alter the shade of both tooth surfaces and resin restorations because of their pronounced pigmentation. As a result, it is crucial to effectively remove the photosensitizers after the PDT of endodontic treatment to prevent any potential adverse effects caused by residual photosensitizers on the teeth of the patients.

Through *in vitro* experiments, researchers examined the efficacy of various treatment protocols (saline, 2.5% sodium hypochlorite, EDTA, passive ultrasonic irrigation (PUI)) in removing MB dye from root canal dentin post-PDT [104]. All protocols exhibited significant cleaning ability on dentin root canals, with the group treated with 2.5% NaClO and PUI showing the most optimal cleaning ability. The excellent removal efficacy of NaClO was attributed to its capability to release oxygen and chlorine, enabling effective cleaning and bleaching of the tooth structure [105]. However, the color residue was still high and remained at a visually perceptible level. Thus, among the tested protocols in this work, no individual solution is entirely effective in eliminating all residual photosensitizer dyes.

In addition, the impact of ultrasonic activation of the final irrigant on the photosensitizer clearing from the root canal wall following PDT treatment was investigated [106]. The study found that combining ultrasonic activation with 17% EDTA and QMix was the most effective in clearing the photosensitizers. QMix was a novel endodontic irrigants containing EDTA, CHX, and surfactant in its composition [107]. The 17% EDTA promoted dentin erosion, which affected the fracture strength of the tooth. In contrast, QMix, although containing EDTA, did not show the ability to promote dentin erosion [108,109]. CHX demonstrated broad-spectrum antimicrobial activity, and surfactants can decrease the surface tension, enhancing the wettability of the solution [110]. Therefore, QMix could serve not only to decontaminate the root canal system but also to promote photosensitizer removal. The removal of the smear layer was also enhanced by the aid of ultrasonic rinsing [111]. The turbulence generated by the ultrasonic device in the solution within the root canal produced cavitation and bubbles. These bubbles, upon colliding with the canal wall, facilitated efficient smear layer elimination [112].

3. PTT

PTT is a photophysical process that converts light energy into thermal energy. When triggered by a particular laser, the photothermal agent produces heat energy through intense intramolecular chemical bond rotation and intermolecular collision [113–118]. PTT, with non-invasiveness and high controllability, has become a promising method widely applied to remove bacterial biofilm from root canals in endodontic treatment [119].

3.1. PTT with a low concentration of irrigants

Firstly, the presence of many tiny branching canals caused by the complex deprogramming structure in the root canal makes it difficult for instruments to access every part of the root canal to eradicate bacteria completely [120]. Secondly, although traditional irrigants, like sodium hypochlorite and CHX, are prevalent in modern RCT, they must be taken in high concentrations to present strong bactericidal ability. The high concentrations of chemical irrigants imply potential unintended infiltration into oral tissues, leading to irreversible damage to periodontal tissues [121]. Moreover, some studies have shown the poor anti-microbial efficacy of traditional irrigants against bacteria in biofilms [122]. Therefore, it is hoped that certain adjunctive methods can be developed to make low-concentration irrigants with desirable therapeutic effects while ensuring high biosafety, and PTT has been considered as a feasible alternative.

To enhance endodontic treatment, PTT agent could be applied together with a low-concentration NaClO solution within the root canal to improve the effectiveness of RCT [57]. Polymer PBDT-IID was synthesized with isoindigo (IID) unit as electron acceptor (A) and benzothiophene unis as electron donor (D), exhibiting an absorption range of 550–750 nm (Figs. 6A and B) [123]. However, the fusion of two IID units into larger fused two isoindigo (DIID) monomers could extend the π-conjugation length and cause an absorption redshift [124]. Therefore, polymer PBDT-DIID was developed with intensive NIR absorption bands between 700 nm and 1000 nm and peak at ~776 nm, indicating a pronounced bathochromic shift (Fig. 6C). Specifically, water-dispersible PBDT-DIID NPs was fabricated by employing the amphiphilic copolymer 1,2-distearoyl-*sn*–glycero-3-phosphoethanolamine-*N*-[methoxy–(polyethylene glycol)−2000] ($DSPE\text{-}PEG_{2000}$) as an encapsulation matrix, and achieved a remarkable photothermal conversion efficiency of 70.6% (Fig. 6D).

The dental pulp was removed using specialized instruments, and the pulp chamber was opened to eliminate necrotic pulp. Following this, PBDT-DIID NPs were mixed into a 1% NaClO solution (10–50 μg/mL) and then administered into the root canal, exposing to an 808 nm laser vertically with 0.5 cm far away from the root canal opening (Fig. 6E). And PBDT-DIID NPs at the concentrations of 25 and 50 μg/mL in 1% NaClO were the most effective in elevating temperature within the root canal. Exploiting extracted human teeth, they developed a root canal infection model, which enabled them to visualize bacterial colonization in the canal using SEM. Within the *E. faecalis* infected root canal model, nearly all bacterial biofilm on the canal surface was eradicated when a 1% NaClO solution was heated using an 808 nm laser.

Furthermore, to assess if the photothermal impact within the root canal might harm the periapical tissue, two sets of teeth were treated: one with a 1% NaClO solution containing PBDT-DIID NPs (50 μg/mL) and the other with a 1% NaClO solution only. Both were subsequently irradiated with 808 nm light for 150 s. The final stained images revealed no notable histopathological changes or lesions in the group containing NPs, indicating that a temperature rise of up 10 °C outside the root canal was not detrimental to adjacent soft tissues. Overall, the photothermal properties of PBDT-DIID were secure and effective and could be used as a means of heating 1% NaClO solution to improve the RCT effect. This research expands the use of photothermal materials in dentistry applications.

3.2. PTT with nanozymes

In addition to serving as a supplementary approach for boosting the anti-bacterial efficacy of low-concentration irrigants, PTT can be synergized with enzyme-mimicking nanomaterials to amplify RCT. And nanozymes exhibit enzyme-like activity by emulating natural enzymes in the innate immune system, capable of ROS generation to degrade cell membranes and various biological macromolecules [125]. However, certain pathogens produce ROS-depleting enzymes and redox-reactive molecules, effectively neutralizing ROS. This significantly reduces the ROS-generation ability of nanozymes to eliminate multi-microbial biofilms [126]. Therefore, the combination of photothermal agents and nanozymes is

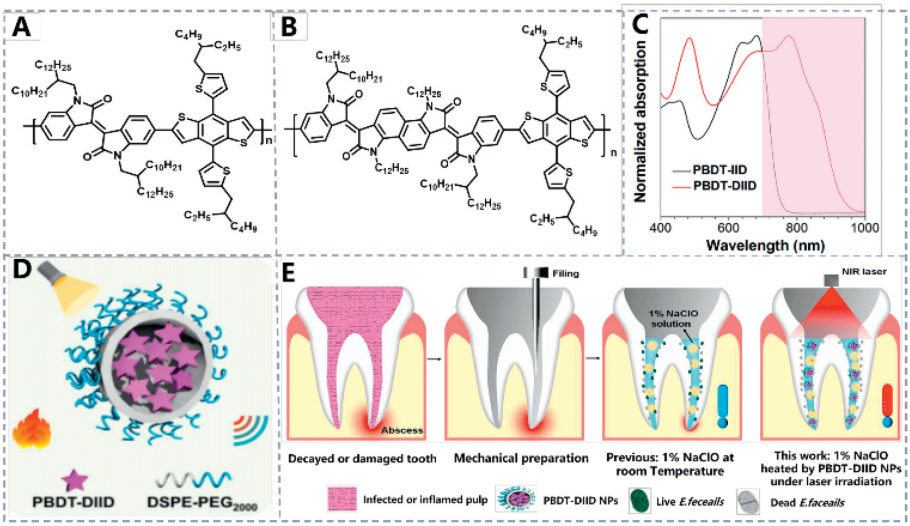

Fig. 6. Molecular structures of π-conjugated polymers (A) PBDT-IID, and (B) PBDT-DIID. (C) Normalized absorbance in tetrahydrofuran (THF). (D) Schematic illustration of PBDT-DIID NPs. (E) RCT process including mechanical preparation and adjunctive sterilization by heating a 1% NaClO solution with PBDT-DIID NPs under 808 nm laser irradiation. Reproduced with permission [57]. Copyright 2021, Wiley-VCH GmbH.

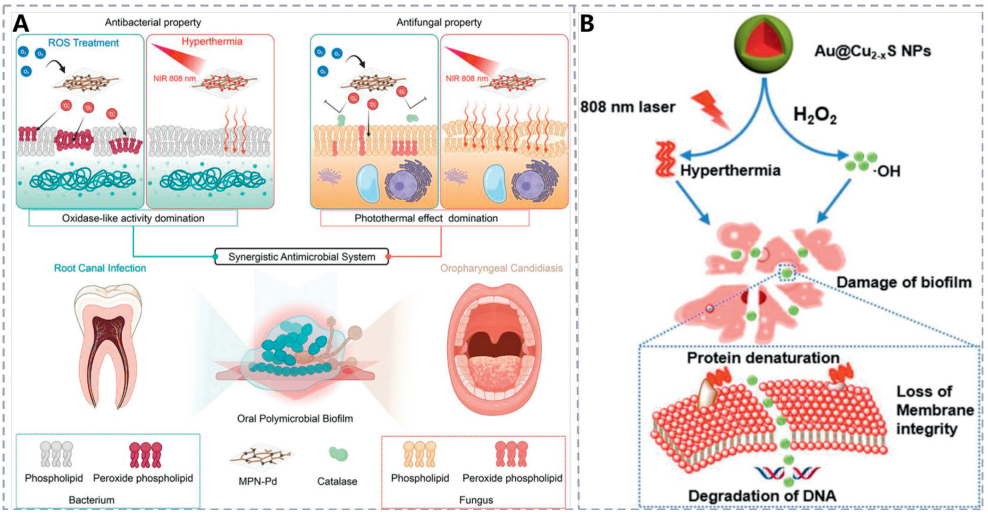

Fig. 7. (A) Schematic of MPN-Pd-mediated anti-microbial nanosystem for oral polymicrobial biofilm-associated infections. Reproduced with permission [58]. Copyright 2023, Wiley-VCH GmbH. (B) PTT combined with peroxidase-like catalytic anti-bacterial of Au@Cu_{2-x}S NPs. Reproduced with permission [59]. Copyright 2021, Elsevier.

considered to be an alternative solution. High temperature enhances cell membrane porosity and deactivates ROS-depleting enzymes, thereby boosting the anti-bacterial efficacy of ROS.

An metal-phenol network featuring Pd nanoparticle nodes (MPN-Pd) was engineered with oxidase-like and photothermal activity to synergistically combat oral multi-microbial biofilm-associated infections more effectively (Fig. 7A) [58]. The $O_2^{\bullet-}$ produced from MPN-Pd was capable of ablating bacteria, such as *S. mutans* and *E. faecalis*, through its oxidase-like properties. *Candida albicans* (*C. albicans*) showed increased sensitivity to high temperatures mediated by MPN-Pd and was eradicated through a photothermal approach. Consequently, the MPN-Pd-driven cooperative anti-bacterial system could swiftly eliminate multi-microbial biofilms from *E. faecalis*, *S. mutans*, and *C. albicans*. Additionally, through the establishment of *in vitro* root canal infection models and *in vivo* oropharyngeal candidiasis studies, the synergistic anti-bacterial efficacy of MPN-Pd against oral biofilm-associated infections was affirmed. This work outlines a practical and achievable approach to the holistic treatment of oral biofilm-associated infections.

In addition, a nano-composite Au@Cu_{2-x}S with integrated NIR photothermal conversion and peroxidase catalytic activities was exploited for synergistic PTT and peroxidase-like catalytic treatment (PCT), to achieve a proficient anti-microbial approach for addressing biofilms during endodontic therapy (Fig. 7B) [59]. The biocompatible Au@Cu_{2-x}S NPs could catalyze the generation of ·OH from H_2O_2 at biosafe concentrations, which could degrade biofilms more effectively than H_2O_2 and CHX.

Moreover, the study on the mechanism of anti-bacterial membranes demonstrated that the nano-composite Au@Cu_{2-x}S notably degraded the primary constituents of biofilms, proteins, and polysaccharides. *In vitro* research showed that the combined effect of free radicals and heat yielded a higher nuclear sterilization rate for Gram-positive *E. faecalis* and Gram-negative *Fusobacterium* nuclei than treatments using either modality alone. Crucially, bactericidal tests using *in vitro* dentures, root canal models, and beagle dog animal models showed that Au@Cu_{2-x}S nano-composite exhibited potent efficacy against bacterial inactivation in biofilms. This research paves the way for a promising, safe, and fast technique to eradicate biofilm-associated bacteria in root canals.

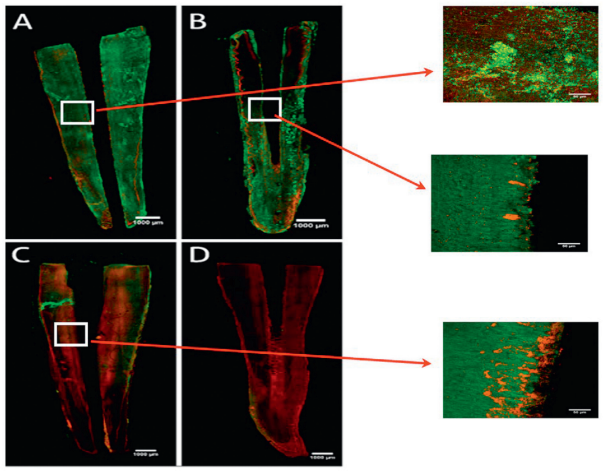

Fig. 8. Confocal laser microscope images of *E. faecalis* biofilm on the root canal surface: (A) untreated, (B) treated with saline + Er,Cr:YSGG, LAI, (C) treated with 0.5% NaClO + LAI, and (D) treated with 5% NaClO + syringe irrigation. Green for viable bacteria, and red for dead bacteria. Copied with permission [60]. Copyright 2019, MDPI.

4. Laser activation irrigation

In addition to photothermal treatment, another way to enhance the effectiveness of anti-biofilm treatment with low concentrations of NaClO is to use laser-activated irrigation (LAI). LAI offers an alternative method for the sanitation and sterilization of the root canal system, demonstrating higher efficacy compared to traditional syringe irrigation or PUI [127]. The operational principle of LAI involves the formation of vacuoles resulting from the intensive absorption of laser energy by water. Er,Cr:YSGG laser activation can induce an immediate turbulent current, leading to the formation of vapor bubbles within the irrigating solution. These bubbles enlarge during the laser pulse and collapse, producing pressure waves capable of generating shear forces along the root canal [128].

The circulation of NaClO within the root canal system enhances the interaction between the active chlorine agents and organic tissues, thus improving the chemical efficacy of the irrigant [129]. The bactericidal effect of LAI improves the removal of the dentin coating layer and aids in removing residues of the root canal [130].

The anti-microbial effect of low concentrations of NaClO, activated by Er,Cr:YSGG laser-activated rinsing, was investigated (Fig. 8) [60]. Most studies have been conducted using biofilms of 24 or 48 h, whereas, in the clinical setting, biofilms that may survive for more extended periods will be encountered. As a result, a 10-day intracanal *E. faecalis* biofilm was employed to simulate natural conditions. The results showed that 0.5% NaClO + Er,Cr:YSGG and 2.5% NaClO + syringe irrigation treatments significantly reduced the number of colony-forming units (CFU)/mm^2. Er,Cr:YSGG LAI was demonstrated to enhance the intra-canal distribution after 60 s of 0.5% NaClO activation, achieving the same effect as 2.5% NaClO. This study holds significant clinical practice, as low concentrations of NaClO can provide both biosafety and desirable therapeutic outcomes.

5. Conclusion and prospects

Through conventional RCT, the intricate nature of the root canal structure makes it challenging to reach effectively, especially for the deeper regions, resulting in recurrent colonization of bacteria within the root canal. And emerging light-induced phototherapy and the construction of nanoplatform, with the features of considerable penetration depth and low drug resistance, is anticipated to break this barrier. Accordingly, this review summarizes the light-responsive nanomaterials and corresponding treatment modalities employed in dental endodontics, including PDT, PTT, and laser-activated irrigation, elucidating the therapeutic mechanisms associated with each modality.

Currently, light-activated therapy is not commonly utilized as the primary method in RCT. It has come to our agreement that light therapy alone is insufficient for complete bacterial eradication from root canals. Instead, it is a supplementary approach to enhance bacterial removal following conventional chemical-mechanical debridement. Therefore, the future implementation of light-activated therapy in clinical RCT is still confronted with various challenges below.

(i) To establish a multi-bacterial biofilm model for real root canal simulation. The validation of the bactericidal effect in many current phototherapy studies primarily focused on a single bacterium, *E. faecalis* biofilm. However, the biofilm in actual root canals typically consists of a diverse bacterial population. Hence, future studies should incorporate a root canal model with multi-species biofilms to experimentally validate the bactericidal efficacy, ensuring the application of the experimental findings from the laboratory to clinical treatment.

(ii) To enhance the drug delivery system for RCT. Light is anticipated to penetrate the depth barrier and reach the innermost regions of the root canal; the complex structure of the canal can impede the effective delivery of light-responsive nano-agents. Hence, in future research, it is essential to explore the development of enhanced delivery systems (*e.g.*, chitosan coatings, nanostructures, ultrasonic activation) to facilitate the deeper penetration of light-responsive nano-agents into the root canal, thereby ensuring comprehensive treatment efficacy. Furthermore, considering the challenge of photosensitizer removal and the potential for tooth staining, the development of photosensitizers with minimal staining activity and ease of removal should be taken into account.

(iii) To explore type I photosensitizers with less oxygen dependence for RCT. The efficacy of RCT relies not only on deep penetration but also on a potent bactericidal effect. PDT using higher concentrations and longer exposure times may still fail to eliminate microorganisms, which is likely attributed to the intricate structure of the root canal combined with the notably low oxygen concentration within the dentin tubules. However, most photosensitizers currently used in endodontic treatment are through type II PDT, which highly relies on oxygen levels. In the future, it is hoped to develop type I PDT with less oxygen dependence, thus improving the PDT efficacy for RCT.

(iv) To develop synergistic therapy for augmenting RCT. Owing to the limitations of each treatment modality, single light-activated therapy may not completely eradicate bacteria from the root canal. Therefore, synergistic treatment with multiple modalities, combining phototherapy with sonodynamic therapy or chemodynamic therapy, is highly desired in the future of RCT to improve the therapeutic efficacy and compensate for the lack of traditional treatments.

Declaration of competing interest

The authors declare that they have no known competing financial interests or personal relationships that could have appeared to influence the work reported in this paper.

CRediT authorship contribution statement

Di An: Writing – review & editing, Writing – original draft, Investigation. **Mingdong She:** Writing – review & editing, Valida-

tion, Investigation. **Ziyang Zhang:** Writing – review & editing, Investigation. **Ting Zhang:** Writing – review & editing, Investigation. **Miaomiao Xu:** Writing – original draft, Investigation. **Jinjun Shao:** Writing – review & editing, Validation, Supervision, Funding acquisition, Conceptualization. **Qian Shen:** Writing – review & editing, Validation, Supervision. **Xuna Tang:** Validation, Supervision.

Acknowledgments

The work was supported by the Natural Science Foundation of Jiangsu Province (No. BK20200092). We are also grateful to the High-Performance Computing Center in Nanjing Tech University for supporting the computational resources.

References

[1] A. Ali, A. Bhosale, S. Pawar, et al., Cureus 14 (2022) e24833.
[2] M.I. Elshinawy, L.A. Al-Madboly, W.M. Ghoneim, et al., Front. Microbiol. 9 (2018) 1371.
[3] O. Feuerstein, Adv. Dent. Res. 24 (2012) 103–107.
[4] D. Sharma, L. Misba, A.U. Khan, Antimicrob. Resist. Infect. Control. 8 (2019) 76.
[5] D.S.W. Benoit, K.R. Sims Jr., D. Fraser, ACS Nano 13 (2019) 4869–4875.
[6] M. Pietiainen, J.M. Liljestrand, R. Akhi, et al., J. Clin. Med. 8 (2019) 889.
[7] A.A. Singh, C.S. Makade, R.J. Krupadam, Mater. Sci. Eng. C 121 (2021) 111864.
[8] M. Wu, H. Shemesh, P.R. Wesselink, Int. Endod. J. 42 (2009) 656–666.
[9] M. Haapasalo, Y. Shen, Z. Wang, et al., Br. Dent. J. 216 (2014) 299–303.
[10] S. Jaju, P.P. Jaju, Int. J. Dent. 2011 (2011) 851359.
[11] S. Stojicic, S. Zivkovic, W. Qian, et al., J. Endod. 36 (2010) 1558–1562.
[12] L. Dotto, R. Sarkis Onofre, A. Bacchi, et al., J. Endod. 46 (2020) 596–604.e3.
[13] H. Tong, Y. Sim, E. Berdouses, et al., Eur. Arch. Paediatr. Dent. 22 (2021) 145–155.
[14] Y. Yan, P. Zhou, H. Lu, et al., Dent. Mater. J. 40 (2021) 986–993.
[15] Z.M. Kanisavaran, Int. Dent. J. 58 (2008) 247–257.
[16] X. Kuang, J. Zhang, X. Peng, et al., J. Oral Microbiol. 13 (2021) 1978756.
[17] Z. Mohammadi, Int. Dent. J. 59 (2009) 35–46.
[18] S. Miglani, N. Tani-Ishii, PeerJ 9 (2021) e11653.
[19] G.Er Karaoglu, Z. Ugur Ydin, D. Erdonmez, et al., Photodiagn. Photodyn. Ther. 32 (2020) 102038.
[20] A. Ghorbanzadeh, M. Aminsobhani, K. Sohrabi, et al., J. Lasers Med. Sci. 7 (2016) 105–111.
[21] R.C.D. Swimberghe, T. Coenye, R.J.G. De Moor, et al., Int. Endod. J. 52 (2019) 604–628.
[22] Q. Shen, L. Wang, X. Ruan, et al., Adv. Funct. Mater. 33 (2023) 2300023.
[23] T. Younas, C. Liu, W.B. Struwe, et al., Small 19 (2023) 2206513.
[24] L. Tu, Y. Xu, Q. Ouyang, et al., Chin. Chem. Lett. 30 (2019) 1731–1737.
[25] S. Cheng, M. Pan, D. Hu, et al., Chin. Chem. Lett. 34 (2023) 108276.
[26] H. Dai, X. Wang, J. Shao, et al., Small 17 (2021) e2102646.
[27] Y. Li, J. Cui, C. Li, et al., Chin. Chem. Lett. 34 (2023) 108180.
[28] G. Feng, G. Zhang, D. Ding, Chem. Soc. Rev. 49 (2020) 8179–8234.
[29] D. Chen, Q. Xu, W. Wang, et al., Small 17 (2021) 2006742.
[30] X. Zhao, J. Liu, J. Fan, et al., Chem. Soc. Rev. 50 (2021) 4185–4219.
[31] F. Hu, S. Xu, B. Liu, Adv. Mater. 30 (2018) 1801350.
[32] G. Plotino, N.M. Grande, M. Mercade, Int. Endod. J. 52 (2019) 760–774.
[33] N. Guo, Y. Xia, Y. Duan, et al., Chin. Chem. Lett. 34 (2023) 107542.
[34] L. Wang, A. Mei, N. Li, et al., Chin. Chem. Lett. 35 (2024) 108974.
[35] W. Hu, P.N. Prasad, W. Huang, Acc. Chem. Res. 54 (2020) 697–706.
[36] H.S. Jung, P. Verwilst, A. Sharma, et al., Chem. Soc. Rev. 47 (2018) 2280.
[37] X. Qu, Y. Hong, H. Cai, et al., Rare Met. 41 (2021) 56–66.
[38] Z. Yali, H. Shuyan, F. Yifen, et al., Coord. Chem. Rev. 455 (2021) 21360.
[39] J. Son, G. Yi, J. Yoo, et al., Adv. Drug Del. Rev. 138 (2018) 133–147.
[40] C. Hu, L. Wang, Y. Lin, et al., Adv. Healthc. Mater. 8 (2019) e1901301.
[41] J. Zhang, H. Chen, M. Zhao, et al., Nano Res. 13 (2020) 2019–2034.
[42] W. Fu, X. Hu, Q. Yuan, et al., Chin. Chem. Lett. 34 (2023) 108064.
[43] H. Wang, Z. Xu, Q. Li, et al., Eng. Regen. 2 (2021) 137–153.
[44] Q. Xu, Y. Yang, J. Lu, et al., Coord. Chem. Rev. 469 (2022) 214687.
[45] L. Yuan, P. Lyu, Y.Y. Huang, et al., J. Photochem. Photobiol. B 203 (2020) 111730.
[46] B. Zong, X. Li, Q. Xu, et al., Front. Microbiol. 13 (2022) 909492.
[47] G. Tenore, G. Palaia, G. Migliau, et al., Appl. Sci. 10 (2020) 2925.
[48] A.A. Balhaddad, Y. Xia, Y. Lan, et al., ACS Nano 15 (2021) 19888–19904.
[49] T. Akbari, M. Pourhajibagher, F. Hosseini, et al., Photodiagn. Photodyn. Ther. 20 (2017) 148–153.
[50] N. Higuchi, J.I. Hayashi, M. Fujita, et al., Int. J. Mol. Sci. 22 (2021) 8384.
[51] F. Ensafi, M. Fazlyab, N. Chiniforush, et al., Photodiagn. Photodyn. Ther. 40 (2022) 103130.
[52] J.M. Sotomil, E.A. Munchow, D. Pankajakshan, et al., J. Endod. 45 (2019) 1371–1377.
[53] M. Pourhajibagher, A. Bahador, Photodiagn. Photodyn. Ther. 39 (2022) 103020.
[54] Y. Qian, Y. Sun, L. Zhang, et al., Adv. Funct. Mater. 34 (2023) 2310636.
[55] X. Zhang, Y. Chen, C. Li, et al., ACS Appl. Bio Mater. 4 (2021) 3796–3804.
[56] J. Chen, H. Zhang, T. Zhao, et al., Adv. Healthc. Mater. 13 (2024) 2302926.
[57] X. Duan, Q. Zhang, Y. Jiang, et al., Adv. Mater. 34 (2022) e2200179.
[58] L. Chen, M. Peng, H. Li, et al., Adv. Mater. 36 (2023) 2306376.
[59] J. Cao, Q. Sun, A.-G. Shen, et al., Chem. Eng. J. 422 (2021) 130090.
[60] P. Betancourt, J.M. Sierra, O. Camps-Font, et al., Antibiotics 8 (2019) 232.
[61] A. Alrahlah, M.O. Niaz, E. Abrar, et al., Photodiagn. Photodyn. Ther. 31 (2020) 101865.
[62] S. Chen, Z. Zhang, L. Wei, et al., Chin. Chem. Lett. 43 (2023) 108412.
[63] L.M. Costa, S. Matos Fde, A.M. Correia, et al., J. Photochem. Photobiol. B 160 (2016) 225–228.
[64] T.J. Whang, H.Y. Huang, M.T. Hsieh, et al., Int. J. Mol. Sci. 10 (2009) 4707–4718.
[65] A.C. Trindade, J.A. De Figueiredo, L. Steier, et al., Photomed. Laser Surg. 33 (2015) 175–182.
[66] Y. Xu, M.J. Young, R.A. Battaglino, et al., J. Endod. 35 (2009) 1567–1572.
[67] S. Carvalho Edos, I. Mello, S.J. Albergaria, et al., Photomed. Laser Surg. 29 (2011) 559–563.
[68] L. Breschi, T. Maravic, S.R. Cunha, et al., Dent. Mater. 34 (2018) 78–96.
[69] T. Phuangkaew, N. Booranabunyat, S. Kiatkamjornwong, et al., Carbohydr. Polym. 277 (2022) 118882.
[70] X. Li, R. Xing, C. Xu, et al., Carbohydr. Polym. 264 (2021) 118050.
[71] M. Pourhajibagher, H. Kazemian, N. Chiniforush, et al., Photodiagn. Photodyn. Ther. 24 (2018) 206–211.
[72] Y. Vendramini, A. Salles, F.F. Portella, et al., Photodiagn. Photodyn. Ther. 32 (2020) 102025.
[73] M.A. Mozayeni, F. Vatandoost, M. Asnaashari, et al., J. Lasers Med. Sci. 11 (2020) S49–S54.
[74] N. Chiniforush, M. Pourhajibagher, S. Shahabi, et al., J. Lasers Med. Sci. 6 (2015) 139–150.
[75] L.Y. Yamamoto, C. Loureiro, L.T.A. Cintra, et al., Photodiagn. Photodyn. Ther. 35 (2021) 102377.
[76] M. Asnaashari, O. Veshveshadi, F. Aslani, et al., Photodiagn. Photodyn. Ther. 43 (2023) 103722.
[77] J. Chen, C. Liu, G. Zeng, et al., Nanoscale Res. Lett. 11 (2016) 85.
[78] F. Cieplik, D. Deng, W. Crielaard, et al., Crit. Rev. Microbiol. 44 (2018) 571–589.
[79] O. Naksuriya, S. Okonogi, R.M. Schiffelers, et al., Biomaterials 35 (2014) 3365–3383.
[80] L.N. Dovigo, A.C. Pavarina, A.P. Ribeiro, et al., Photochem. Photobiol. 87 (2011) 895–903.
[81] D. Rai, J.K. Singh, N. Roy, et al., Int. J. Biol. Macromol. 410 (2008) 147–155.
[82] G. Sivieri-Araujo, H.B. Strazzi-Sahyon, D.P. Jacomassi, et al., Photodiagn. Photodyn. Ther. 37 (2022) 102650.
[83] H.A. Ricci Donato, S. Pratavieira, C. Grecco, et al., Photomed. Laser Surg. 35 (2017) 105–110.
[84] S.V. Berwin Singh, E. Jung, J. Noh, et al., Nanomedicine 16 (2019) 45–55.
[85] S. Jiang, R. Zhu, X. He, et al., Int. J. Nanomed. 12 (2017) 167–178.
[86] V. Kushwaha, R.K. Yadav, A.P. Tikku, et al., J. Clin. Exp. Dent. 10 (2018) e1155–e1160.
[87] A. Lloyd, J.P. Uhles, D.J. Clement, et al., J. Endod. 40 (2014) 584–587.
[88] A. Erkiert-Polguj, A. Halbina, I. Polak-Pacholczyk, et al., J. Cosmet. Laser Ther. 18 (2016) 105–110.
[89] K. Chachlioutaki, C. Karavasili, E. Adamoudi, et al., ACS Biomater. Sci. Eng. 8 (2022) 2096–2110.
[90] M. Nowak-Perlak, M.A. Bromke, P. Ziolkowski, et al., Int. J. Mol. Sci. 23 (2022) 6276.
[91] E. Polat, K. Kang, Biomedicines 9 (2021) 584.
[92] P. Li, F. Wen, H. Yan, et al., LWT Food Sci. Technol. 181 (2023) 114750.
[93] M. Pourhajibagher, B. Rahimi-Esboei, H. Ahmadi, et al., Photodiagn. Photodyn. Ther. 34 (2021) 102288.
[94] F. Zhang, R. Li, C. Xu, et al., Phytomedicine 95 (2022) 153786.
[95] J. Yuhan, L. Zhu, L. Zhu, et al., J. Control. Release 346 (2022) 405–420.
[96] Y.A. Hashem, K.A. Abdelrahman, R.K. Aziz, Infect. Drug Resist. 14 (2021) 1713–1723.
[97] D. Bartusik-Aebisher, Ł. Ożóg, W. Domka, et al., Photochem. Photobiol. 97 (2021) 1445–1452.
[98] S. Demartis, A. Obinu, E. Gavini, et al., Dyes Pigm. 188 (2021) 109236.
[99] L. Luo, L. Yan, A. Amirshaghaghi, et al., ACS Appl. Bio Mater. 3 (2020) 2344–2349.
[100] Y. Wang, T. Zhang, X. Liang, Small 12 (2016) 6634 -6634.
[101] D. Chen, Z. Zhong, Q. Ma, et al., ACS Appl. Mater. Interfaces 12 (2020) 26914–26925.
[102] D. Chen, C. Liang, X. Qu, et al., Biomaterials 292 (2023) 121944.
[103] A. Shahravan, A.A. Haghdoost, A. Adl, et al., J. Endod. 33 (2007) 96–105.
[104] K.M. Ramalho, S.R. Cunha, E. Mayer-Santos, et al., Photodiagn. Photodyn. Ther. 20 (2017) 248–252.
[105] M. Zehnder, J. Endod. 32 (2006) 389–398.
[106] M.A. Souza, B. Pazinatto, K.F. Bischoff, et al., Photodiagn. Photodyn. Ther. 17 (2017) 216–220.
[107] S. Stojicic, Y. Shen, W. Qian, et al., Int. Endod. J. 45 (2012) 363–371.
[108] M.A. Saghiri, A. Delvarani, P. Mehrvarzfar, et al., Oral Surg. Oral Med. Oral Pathol. Oral Radiol. Endod. 108 (2009) e29–e34.
[109] D.E. Bottcher, N.T. Sehnem, F. Montagner, et al., J. Endod. 41 (2015) 1364–1370.
[110] L. Giardino, E. Ambu, C. Becce, et al., J. Endod. 32 (2006) 1091–1093.
[111] G. Caron, K. Nham, F. Bronnec, et al., J. Endod. 36 (2010) 1361–1366.
[112] E.M. Ribeiro, Y.T. Silva-Sousa, A.E. Souza-Gabriel, et al., Microsc. Res. Tech. 75 (2012) 781–790.
[113] X. Li, J.F. Lovell, J. Yoon, et al., Nat. Rev. Clin. Oncol. 17 (2020) 657–674.

[114] X. Cui, Q. Ruan, X. Zhuo, et al., Chem. Rev. 123 (2023) 6891–6952.
[115] W. Wang, Q. Shen, H. Cai, et al., Nano Res. 16 (2022) 117–126.
[116] X. Ruan, M. Wei, X. He, et al., Colloids Surf. B. Biointerfaces 231 (2023) 113547.
[117] H. Dai, Z. Cheng, T. Zhang, et al., Chin. Chem. Lett. 33 (2021) 2501–2506.
[118] K. Xu, M. Guo, X. Sun, et al., Sens. Actuat. B: Chem. 401 (2023) 135091.
[119] B. Bolhari, N. Meraji, R. Seddighi, et al., Photodiagn. Photodyn. Ther. 42 (2023) 103345.
[120] J. Li, W. Zhang, W. Ji, et al., J. Mater. Chem. B 9 (2021) 7909–7926.
[121] A. Segu, D. Bijukumar, T. Trinh, et al., ACS Biomater. Sci. Eng. 4 (2018) 2623–2632.
[122] H. Takahashi, E.T. Nadres, K. Kuroda, Biomacromolecules 18 (2017) 257–265.
[123] K. Chang, Y. Liu, D. Hu, et al., ACS Appl. Mater. Interfaces 10 (2018) 7012–7021.
[124] Y. Jiang, X. Zheng, Y. Deng, et al., Angew. Chem. Int. Ed. 57 (2018) 10283–10287.
[125] C. Cao, N. Yang, X. Wang, et al., Coord. Chem. Rev. 491 (2023) 215245.
[126] P. Dong, Y. Zhan, S. Jusuf, et al., Adv. Sci. 9 (2022) 2104384.
[127] J. Guo, Y. Xu, M. Liu, et al., J. Mater. Chem. B 9 (2021) 7686–7697.
[128] P. Betancourt, A. Merlos, J.M. Sierra, Photobiomodul. Photomed. Laser Surg. 38 (2020) 91–97.
[129] R.G. Macedo, P.R. Wesselink, F. Zaccheo, et al., Int. Endod. J. 43 (2010) 1108–1115.
[130] S.D. de Groot, B. Verhaagen, M. Versluis, et al., Int. Endod. J. 42 (2009) 1077–1083.